P-ISSN 2586-9000
E-ISSN 2586-9027
Homepage : https://tci-thaijo.org/index.php/SciTechAsia
Science & Technology Asia
Vol.28 No.4 October - December 2023
Page: [67-85]
Original research article

Mathematical Modeling and Optimal Control of HPV Infection of Epithelial Cells and Cervical Cancer

Ratchada Viriyapong*, Naratip Junphom

Department of Mathematics, Faculty of Science, Naresuan University, Phitsanulok 65000, Thailand

Received 23 August 2023; Received in revised form 26 October 2023
Accepted 15 November 2023; Available online 27 December 2023

ABSTRACT

In this paper, a within-host model of human papillomavirus (HPV) infection and cervical cancer is proposed. The model consists of seven compartments including susceptible, exposed, infected, early-stage cervical cancer cells, end-stage cervical cancer cells, HPV, and recovered cervical cells. The existence, positivity and boundary of solutions are proved and the basic reproduction number is calculated. We obtain that when the basic reproduction number is less than one, an infection-free equilibrium point is both locally and globally stable, whereas when it is greater than one an infected steady state exists and is globally stable. Further, the optimal control problem is applied in this study by using Pontryagin's Minimum Principle with three control variables which are preventive vaccine, treatment effort for infected cervical cells and treatment effort for early-stage cervical cancer cells. Numerical simulations of optimal control model demonstrate that each individual control could reduce an HPV infection and cervical cancer to some certain extent, however, a combination of all three controls gives the best scenario in controlling HPV infection and cervical cancer.

Keywords: Cervical cancer; Epithelial cell; HPV infection; Optimal control; Treatment; Vaccination

1. Introduction

Human papillomavirus (HPV) is considered as one of the viruses that contribute to the cancer and other disease. It is one of the most common causes of sexual transmitted infection worldwide. HPV is a double-stranded DNA virus in Papovaviridae family that infects epithelium [1-3]. There are more than 200 types of HPVs that are identified where the high-risk types are 16, 18, 31, 33, 35, 39, 45. 51, 52, 56, 58, 59 and 68 [2]. About

*Corresponding author: ratchadapa@nu.ac.th
doi: 10.14456/scitechasia.2023.72

50% of all patients with cervical cancers worldwide are associated with HPV 16 [3, 4]. Infection with high-risk HPV type could develop further to cervical cancer although it is not sufficient to cause cancer by itself [3, 5]. Most HPV infections are benign, however, persistent infection can cause cervical cancer in woman [6].

Cervical cancer is the fourth most common cancer among women worldwide. According to World Health Organization (WHO), globally in 2020 approximately 604,000 women were diagnosed with cervical cancer and about 342,000 women died from the disease [6]. However, cervical cancer is one of cancer related diseases that can be cured and treated successfully if diagnosed early and treated promptly.

HPV infected cells can be eliminated over time without any treatment although when the infection persists, one can be treated by medications, surgical and other procedures. Further, any precancerous lesions needed to be removed together with other procedures. HPV infection can be prevented by HPV vaccine which helps in protecting us against some certain types of HPV which could lead to genital warts or cancer. According to work by Brotherton, 2019, the statistical data shows that HPV vaccine utilization is very effective in preventing infection and disease related to the specific HPV genotypes [7]. In many countries worldwide, vaccine programs have been very successful [7, 8].

As with many other diseases, mathematical models have been a useful tool to further and better understanding of HPV infection and cervical cancer. Models at population level have been studied by a number of researchers. The examples are the work by Elbasha, 2008 [9], Ribassin-Majed and Lounes, 2010 [10] and Lee and Tameru, 2012 [11]. Further, optimal control was also applied into the model to seek the appropriate strategy to control the HPV infection, e.g., the work by Gurmu et al., 2019 [12], Zhang et al., 2020a [13] and Zhang et al., 2020b [14].

In addition, some researchers studied the HPV infection further at the molecular level to understand the necessary interactions of viruses spreading within cells. To our knowledge, there are only a few works that investigate within-host dynamics of HPV infection. In 2015, Smith et al. proposed a within-host model to examine the long-term outcomes of HPV vaccination and they divided cells into two types which are low-risk and high-risk [15]. A year later, Asih et al. proposed a model which involves free virus compartment and the cells were divided into four compartments i.e., susceptible, infected, precancerous and cancer cells [16]. In 2019, Gurmu and Koya proposed a model to study the impact of screening on HPV transmission. Their model consists of five compartments i.e., susceptible, unaware infected, screened infected, recovered and cervical cancer cells [17]. Recently, Allali had extended the work of Asih et al., 2016 by adding two therapies i.e., therapy for blocking new infection and therapy for inhibiting viral production [18] and also considered optimal control into his model.

In this study, we therefore propose a within-host model of HPV infection and cervical cancer. Our model includes the latent period of HPV infection and considers two different stages of cancer i.e., early-stage and end-stage and the recover cervical cells. Later on, optimal control has been applied into our model with three control variables in order to seek the appropriate strategy to control HPV infection and cervical cancer. The paper is constructed as follows. We start describing how our model is for-

mulated in section 2. All model properties are demonstrated and proved in section 3. The optimal control model is in section 4, where its numerical simulations are shown in section 5. Finally, we briefly discuss our results and conclude in section 6.

2. Model Formulation

In this study, we propose a within-host model of HPV infection and cervical cancer. We extend the work of Asih et al., 2016 [16] by adding the latent period of HPV infection and the recovery state of cells. Our model consists of seven compartments which are S is the concentration of susceptible cervical cells, E is the concentration of exposed cervical cells, I is the concentration of infected cervical cells, C_1 is the concentration of early-stage cervical cancer cells, C_2 is the concentration of end-stage cervical cancer cells, V is the concentration of human papillomavirus (HPV) and R is the concentration of recovered cells. The cervical cells are recruited at a rate Λ, they are infected by both viruses and infected cervical cells at a rate β giving the transmission term as $\beta S(V + I)$. Once the cervical cells are infected, they first are in the exposed state then are transferred to infected state at a rate ω. Both exposed and infected cervical cells can be recovered with a rate q and α, respectively, whereas some of infected cervical cells progress to become early-stage cervical cancer cells at a rate δ. The cancer cells at this early stage can be recovered by some treatment at a rate ϕ and can progress to become end-stage cervical cancer cells at a rate θ. All cervical cells die naturally at a rate μ, whereas the infected cervical cells die at a rate d due to the HPV infection and both early-stage cervical cancer cells and end-stage cervical cancer cells die due to the cancer at a rate ρ and m, respectively. Further, HPVs are generated at a rate k by infected cervical cells and are cleared at a rate ϵ. The diagram of model described above is shown in Fig. 1.

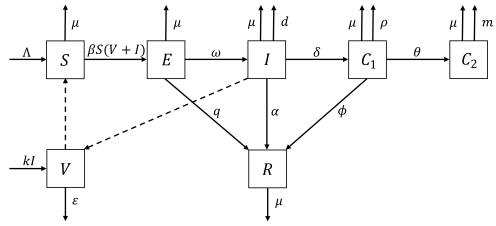

Fig. 1. A schematic diagram for the HPV infection and cervical cancer of epithelial cells model.

The model above is given by the following system of differential equations:

$$\begin{aligned}
\frac{dS}{dt} &= \Lambda - \mu S - \beta S(V + I),\\
\frac{dE}{dt} &= \beta S(V + I) - (\mu + \omega + q)E,\\
\frac{dI}{dt} &= \omega E - (\mu + d + \delta + \alpha)I,\\
\frac{dC_1}{dt} &= \delta I - (\mu + \rho + \theta + \phi)C_1, \qquad (2.1)\\
\frac{dC_2}{dt} &= \theta C_1 - (\mu + m)C_2,\\
\frac{dV}{dt} &= kI - \epsilon V,\\
\frac{dR}{dt} &= qE + \alpha I + \phi C_1 - \mu R,
\end{aligned}$$

with initial conditions: $S(0) \geq 0$, $E(0) \geq 0$, $I(0) \geq 0$, $C_1(0) \geq 0$, $C_2(0) \geq 0$, $V(0) \geq 0$, $R(0) \geq 0$.

Here, the population of all cervical cells are represented by $N(t) = S(t)+E(t)+I(t) + C_1(t) + C_2(t) + R(t)$.

3. Model Analysis

3.1 Model properties

3.1.1 Existence of solution

Theorem 3.1. *Let* $S_0, E_0, I_0, C_{1_0}, C_{2_0}, V_0, R_0 \in \mathbb{R}$ *be given. There exists*

$t_0 > 0$ *and continuously differentiable functions* $S, E, I, C_1, C_2, V, R : [0, t_0) \longrightarrow \mathbb{R}$ *such that the ordered* $(S, E, I, C_1, C_2, V, R)$ *satisfies the system (2.1) and* $(S, E, I, C_1, C_2, V, R)(0) = (S_0, E_0, I_0, C_{1_0}, C_{2_0}, V_0, R_0)$.

Proof. We use the classical $Picard - Lindelöf$ theorem to prove. First, let

$$f = \begin{bmatrix} \Lambda - \mu S - \beta S(V+I) \\ \beta S(V+I) - (\mu + \omega + q)E \\ \omega E - (\mu + d + \delta + \alpha)I \\ \delta I - (\mu + \rho + \theta + \phi)C_1 \\ \theta C_1 - (\mu + m)C_2 \\ kI - \epsilon V \\ qE + \alpha I + \phi C_1 - \mu R \end{bmatrix}. \quad (3.1)$$

We next calculate all partial derivatives of f to show that they are continuous and bounded. Thus, the Jacobian matrix of f is

$$J(f) = \begin{bmatrix} -\mu - \beta(V+I) & 0 & -\beta S & 0 & 0 & 0 & 0 \\ \beta(V+I) & -(\mu + \omega + q) & \beta S & 0 & 0 & 0 & 0 \\ 0 & \omega & -(\mu + d + \delta + \alpha) & 0 & 0 & 0 & 0 \\ 0 & 0 & \delta & -(\mu + \rho + \theta + \phi) & 0 & 0 & 0 \\ 0 & 0 & 0 & \theta & -(\mu + m) & 0 & 0 \\ 0 & 0 & 0 & 0 & 0 & -\epsilon & 0 \\ 0 & q & \alpha & \phi & 0 & 0 & -\mu \end{bmatrix}. \quad (3.2)$$

The $J(f)$ above is linear and therefore it is locally bounded for every $(S, E, I, C_1, C_2, V, R) \in \mathbb{R}^7$. Hence, f has a continuous and bounded derivative on any compact subset of $\mathbb{R}^7$. This leads to f being locally Lipschitz in $\mathbb{R}^7$. Therefore, by the $Picard - Lindelöf$ Theorem [19], there exists a unique solution of system (2.1) with initial value $(S_0, E_0, I_0, C_{1_0}, C_{2_0}, V_0, R_0)$ on $[0, t_0]$ for some $t_0 > 0$. □

3.1.2 Positivity and boundedness of the solutions

Theorem 3.2. *With nonnegative initial conditions, all solutions of system (2.1) remain nonnegative and bounded for all* $t > 0$.

Proof. For $t > 0$, we have the following :

$$\left.\frac{dS}{dt}\right|_{S=0} = \Lambda \geq 0, \quad (3.3)$$

$$\left.\frac{dE}{dt}\right|_{E=0} = \beta S(V+I) \geq 0, \quad (3.4)$$

$$\left.\frac{dI}{dt}\right|_{I=0} = \omega E \geq 0, \quad (3.5)$$

$$\left.\frac{dC_1}{dt}\right|_{C_1=0} = \delta I \geq 0, \quad (3.6)$$

$$\left.\frac{dC_2}{dt}\right|_{C_2=0} = \theta C_1 \geq 0, \quad (3.7)$$

$$\left.\frac{dV}{dt}\right|_{V=0} = kI \geq 0, \quad (3.8)$$

$$\left.\frac{dR}{dt}\right|_{R=0} = qE + \alpha I + \phi C_1 \geq 0. \quad (3.9)$$

Therefore, by functional differential equations theory, the positivity of all solutions initiating in $\mathbb{R}^7_+$ is guaranteed for all $t > 0$. Next, we will prove the boundedness of solutions. □

Since $N(t) = S(t) + E(t) + I(t) + C_1(t) + C_2(t) + R(t)$, then

$$\begin{aligned} \frac{dN}{dt} &= \Lambda - \mu(S + E + I + C_1 + C_2 + R) \\ &\quad - dI - \rho C_1 - mC_2 \\ &\leq \Lambda - \mu(S + E + I + C_1 + C_2 + R) \\ &\leq \Lambda - \mu N. \end{aligned} \quad (3.10)$$

Then, we have

$$\frac{dN}{dt} + \mu N \leqslant \Lambda. \quad (3.11)$$

We next solve Eq. (3.11) by using integrating factor $(I.F)$, where $I.F = e^{\mu t}$. Multiplying both sides of Eq. (3.11) by the above $I.F$, we have

$$e^{\mu t}\left(\frac{dN}{dt} + \mu N\right) \leqslant \Lambda e^{\mu t}. \quad (3.12)$$

The Eq. (3.12) can be written as

$$\frac{d}{dt}\left(N(t)e^{\mu t}\right) \leqslant \Lambda e^{\mu t}. \quad (3.13)$$

Integrating both sides of Eq. (3.13), then

$$N(t) \leqslant \frac{\Lambda}{\mu} - \left(\frac{\Lambda}{\mu} - N(0)\right)e^{-\mu t}. \quad (3.14)$$

Then, $N(t) \to \frac{\Lambda}{\mu}$ as $t \to \infty$, implying $N_1(t) \in \left(0, \frac{\Lambda}{\mu}\right]$.

Hence, $N(t)$ is bounded above by $\frac{\Lambda}{\mu}$.

By the above method, we then have

$$V(t) \leqslant \frac{k\Lambda}{\epsilon\mu} - \left(\frac{k\Lambda}{\epsilon\mu} - V(t)\right)e^{\epsilon t}. \quad (3.15)$$

Then, $V(t) \to \frac{k\Lambda}{\epsilon\mu}$ as $t \to \infty$, implying $V(t) \in \left(0, \frac{k\Lambda}{\epsilon\mu}\right]$.

Hence, $V(t)$ is bounded above by $\frac{k\Lambda}{\epsilon\mu}$.

Hence, all solutions of system (2.1) are bounded and the biologically feasible region Ω for system (2.1) is defined by the following compact set

$$\Omega = \left\{(S, E, I, C_1, C_2, V, R) \in \mathbb{R}^7_+ : N \leq \frac{\Lambda}{\mu} \text{ and } V \leq \frac{k\Lambda}{\epsilon\mu}\right\}.$$

This completes the proof.

3.2 Infection-free equilibrium point

The infection-free equilibrium point is

$$IFE = (S_0^*, E_0^*, I_0^*, C_{1_0}^*, C_{2_0}^*, V_0^*, R_0^*) = \left(\frac{\Lambda}{\mu}, 0, 0, 0, 0, 0, 0\right). \quad (3.16)$$

3.3 The basic reproduction number $\mathcal{R}_0$

The basic reproduction number ($\mathcal{R}_0$) is the expected number of secondary cases of HPV infection caused by a typical case of infected cell. The next-generation matrix method by [20] is used to calculate $\mathcal{R}_0$. Matrices $\mathcal{F}$ and $\mathcal{V}$ are obtained below, where $\mathcal{F}$ is the matrix of the rate of appearance of new infections and $\mathcal{V}$ is the matrix of the transfer rate of individual infections.

$$\mathcal{F} = \begin{bmatrix} \beta S(V+I) \\ 0 \\ 0 \end{bmatrix},$$

and

$$\mathcal{V} = \begin{bmatrix} (\mu+\omega+q)E \\ (\mu+d+\delta+\alpha)I - \omega E \\ \epsilon V - kI \end{bmatrix}.$$

The Jacobian matrices of $\mathcal{F}$ and $\mathcal{V}$ are

$$F = \begin{bmatrix} 0 & \beta S & \beta S \\ 0 & 0 & 0 \\ 0 & 0 & 0 \end{bmatrix},$$

and

$$V = \begin{bmatrix} (\mu+\omega+q) & 0 & 0 \\ -\omega & (\mu+d+\delta+\alpha) & 0 \\ 0 & -k & \epsilon \end{bmatrix}.$$

By $IFE = \left(\frac{\Lambda}{\mu}, 0, 0, 0, 0, 0, 0\right)$, one has

$$F(E_0) = \begin{bmatrix} 0 & \beta\frac{\Lambda}{\mu} & \beta\frac{\Lambda}{\mu} \\ 0 & 0 & 0 \\ 0 & 0 & 0 \end{bmatrix},$$

and

$$V(E_0) = \begin{bmatrix} (\mu+\omega+q) & 0 & 0 \\ -\omega & (\mu+d+\delta+\alpha) & 0 \\ 0 & -k & \epsilon \end{bmatrix}.$$

And,

$$FV^{-1} = \begin{bmatrix} \frac{\beta\Lambda\omega(\epsilon+k)}{\mu\epsilon(\mu+\omega+q)(\mu+d+\delta+\alpha)} & \frac{\beta\Lambda(\epsilon+k)}{\mu\epsilon(\mu+d+\delta+\alpha)} & \frac{\beta\Lambda}{\mu\epsilon} \\ 0 & 0 & 0 \\ 0 & 0 & 0 \end{bmatrix}.$$

The basic reproduction number is given by the spectral radius of the martrix FV^{-1}, thus

$$\mathcal{R}_0 = \frac{\beta\Lambda\omega(\epsilon+k)}{\mu\epsilon(\mu+\omega+q)(\mu+d+\delta+\alpha)}.$$

3.4 The infected steady state

The infected steady state is denoted by $E_1^* = (S^*, E^*, I^*, C_1^*, C_2^*, V^*, R^*)$ where

$$S^* = \frac{(\mu+\omega+q)(\mu+d+\delta+\alpha)}{\beta\omega(\frac{k}{\epsilon}+1)},$$
$$E^* = \frac{(\mu+d+\delta+\alpha)}{\omega}I^*,$$
$$I^* = \frac{\mu\epsilon}{\beta(k+\epsilon)}[R_0-1],$$
$$C_1^* = \frac{\delta}{(\mu+\rho+\theta+\phi)}I^*,$$
$$C_2^* = \frac{\theta\delta}{(\mu+m)(\mu+\rho+\theta+\phi)}I^*,$$
$$V^* = \frac{k}{\epsilon}I^*,$$
$$R^* = \left[\frac{\frac{q(\mu+d+\delta+\alpha)}{\omega}+\alpha+\frac{\phi\delta}{(\mu+\rho+\theta+\phi)}}{\mu}\right]I^*.$$

3.5 Stability of infection-free equilibrium point

3.5.1 Local stability of infection-free equilibrium point

Theorem 3.3. *If $R_0 < 1$, then the infection-free equilibrium point (IFE) is locally asymptotically stable, otherwise it is unstable.*

Proof. The Jacobian matrix of the infection-free equilibrium point is

$$J\left(S_0^*, E_0^*, I_0^*, C_{1_0}^*, C_{2_0}^*, V_0^*, R_0^*\right) = \begin{bmatrix} -\mu & 0 & -\frac{\beta\Lambda}{\mu} \\ 0 & -(\mu+\omega+q) & \frac{\beta\Lambda}{\mu} \\ 0 & \omega & -(\mu+d+\delta+\alpha) \\ 0 & 0 & \delta \\ 0 & 0 & 0 \\ 0 & 0 & k \\ 0 & q & \alpha \end{bmatrix}$$

$$\begin{bmatrix} 0 & 0 & -\frac{\beta\Lambda}{\mu} & 0 \\ 0 & 0 & \frac{\beta\Lambda}{\mu} & 0 \\ 0 & 0 & 0 & 0 \\ -(\mu+\rho+\theta+\phi) & 0 & 0 & 0 \\ \theta & -(\mu+m) & 0 & 0 \\ 0 & 0 & -\epsilon & 0 \\ \phi & 0 & 0 & -\mu \end{bmatrix}.$$

Then, we find the eigenvalues by determining the characteristic equation as follows:

$$det(J(IFE) - \lambda I) = 0,$$

$$\begin{vmatrix} -\mu-\lambda & 0 & -\frac{\beta\Lambda}{\mu} \\ 0 & -(\mu+\omega+q)-\lambda & \frac{\beta\Lambda}{\mu} \\ 0 & \omega & -(\mu+d+\delta+\alpha)-\lambda \\ 0 & 0 & \delta \\ 0 & 0 & 0 \\ 0 & 0 & k \\ 0 & q & \alpha \end{vmatrix}$$

$$\begin{vmatrix} 0 & 0 & -\frac{\beta\Lambda}{\mu} & 0 \\ 0 & 0 & \frac{\beta\Lambda}{\mu} & 0 \\ 0 & 0 & 0 & 0 \\ -(\mu+\rho+\theta+\phi)-\lambda & 0 & 0 & 0 \\ \theta & -(\mu+m)-\lambda & 0 & 0 \\ 0 & 0 & -\epsilon-\lambda & 0 \\ \phi & 0 & 0 & -\mu-\lambda \end{vmatrix} = 0.$$

Hence, the first four eigenvalues are

$$\lambda_1 = -\mu < 0,$$
$$\lambda_2 = -\mu < 0,$$
$$\lambda_3 = -(\mu+m) < 0,$$
$$\lambda_4 = -(\mu+\rho+\theta+\phi) < 0.$$

And, the rest of a characterestic equation is

$$\lambda^3 + \Big((\mu+\omega+q)+(\epsilon+\mu+d+\delta+\alpha)\Big)\lambda^2$$
$$+\Big((\mu+\omega+q)(\epsilon+\mu+d+\delta+\alpha)+\epsilon(\mu+d+\delta+\alpha)-\frac{\beta\Lambda\omega}{\mu}\Big)\lambda$$
$$+\Big(\epsilon(\mu+\omega+q)(\mu+d+\delta+\alpha)-\frac{\beta\Lambda\omega(\epsilon+k)}{\mu}\Big) = 0.$$

Consider the above characteristic equation by using the Routh-Hurwitz Criterion and consider it in the form of

$$\lambda^3 + a_1\lambda^2 + a_2\lambda + a_3 = 0,$$

we have

$$a_1 = (\mu+\omega+q)+(\epsilon+\mu+d+\delta+\alpha) > 0,$$
$$a_3 = \epsilon(\mu+\omega+q)(\mu+d+\delta+\alpha)\left[1-\frac{\beta\Lambda\omega(\epsilon+k)}{\mu\epsilon(\mu+\omega+q)(\mu+d+\delta+\alpha)}\right]$$
$$= \epsilon(\mu+\omega+q)(\mu+d+\delta+\alpha)\Big[1-R_0\Big],$$

when $\mathcal{R}_0 < 1$ then $a_3 > 0$

$$a_1a_2 - a_3 = \Big[(\mu+\omega+q)+(\epsilon+\mu+d+\delta+\alpha)\Big]\cdot$$

$$\Big[(\mu+\omega+q)(\epsilon+\mu+d+\delta+\alpha)-\tfrac{\beta\Lambda\omega}{\mu}\Big]$$
$$+\epsilon(\mu+d+\delta+\alpha)\Big[(\mu+\omega+q)+(\epsilon+\mu+d+\delta+\alpha)\Big]$$
$$-\epsilon(\mu+\omega+q)(\mu+d+\delta+\alpha)\Big[1-R_0\Big].$$

Consider when $\mathcal{R}_0 < 1$, we have

$$\epsilon(\mu+\omega+q)(\mu+d+\delta+\alpha)$$
$$> \epsilon(\mu+\omega+q)(\mu+d+\delta+\alpha)\Big[1-R_0\Big],$$

and

$$\frac{\beta\Lambda\omega(\epsilon+k)}{\mu\epsilon} < (\mu+\omega+q)(\mu+d+\delta+\alpha).$$

This implies that

$$\frac{\beta\Lambda\omega}{\mu} \leqslant \frac{\beta\Lambda\omega(\epsilon+k)}{\mu\epsilon} < (\mu+\omega+q)(\mu+d+\delta+\alpha)$$
$$\leqslant (\mu+\omega+q)(\epsilon+\mu+d+\delta+\alpha).$$

Thus $a_1a_2 - a_3 > 0$, i.e., $a_1a_2 > a_3$ when $\mathcal{R}_0 < 1$. Therefore, we obtain that when $\mathcal{R}_0 < 1$, then $a_1 > 0, a_3 > 0$ and $a_1a_2 > a_3$. Thus, by the Routh-Hurwitz Criterion, the infection-free equilibrium point is locally asymptotically stable, if $\mathcal{R}_0 < 1$. When $\mathcal{R}_0 > 1$, it is unstable. This completes the proof. □

3.5.2 Global stability of the infection-free equilibrium point

In this subsection, we use a method of Castillo-Chavez et al. [21] by considering a model system written in the form

$$\frac{dX_1}{dt} = F(X_1, X_2),$$
$$\frac{dX_2}{dt} = G(X_1, X_2), \quad G(X_1, 0) = 0,$$

where $X_1 \in \mathbb{R}^m$ denotes (its components) the number of uninfected individuals and $X_2 \in \mathbb{R}^n$ denotes (its components) the number of infected individuals including latent, infectious, etc; (X_1^*) denotes the infection-free equilibrium of the system. Also assume the conditions (H1) and (H2) below:

(H1) For $\frac{dX_1}{dt} = F(X_1, 0)$, X_1^* is globally asymptotically stable,

(H2) $G(X_1, X_2) = AX_2 - \hat{G}(X_1, X_2)$, all elements in $\hat{G}(X_1, X_2)$ are nonnegative for$(X_1, X_2) \in \Omega$,

where the Jacobian $A = \frac{\partial G}{\partial X_2}(X_1^*, 0)$ is an M-matrix (the off diagonal elements of A are nonnegative) and Ω is the region where the model makes biological sense.
Then the IFE is globally asymptotically stable provided that $\mathcal{R}_0 < 1$.

Theorem 3.4. *(global stability of IFE). If $\mathcal{R}_0 < 1$, then IFE is globally asymptotically stable.*

Proof. To show that the conditions (H1) and (H2) hold when $\mathcal{R}_0 < 1$. In our ODE system, we let $X_1 = (S, R), X_2 = (E, I, C_1, C_2, V)$ and $X_1^* = \left(\frac{\Lambda}{\mu}, 0\right)$.
Therefore,

$$\frac{dX_1}{dt} = F(X_1, X_2) = \begin{bmatrix} \Lambda - \mu S - \beta S(V+I) \\ qE + \alpha I + \phi C_1 - \mu R \end{bmatrix}.$$

We have

$$\frac{dX_1}{dt} = F(X_1, 0) = \begin{bmatrix} \Lambda - \mu S \\ -\mu R \end{bmatrix}.$$

From above, we have $\frac{dS}{dt} = \Lambda - \mu S$.
By solving above differential equation, we obtain

$$S_t = \frac{\Lambda}{\mu} - \frac{(\Lambda - \mu S_0)e^{-\mu t}}{\mu}.$$

Consider when $t \longrightarrow \infty$, then $S(t) \longrightarrow \frac{\Lambda}{\mu}$.
Similarly, we have from above that

$$\frac{dR}{dt} = -\mu R.$$

Thus, $R_t = R_0 e^{-\mu t}$.
Consider when $t \longrightarrow \infty$, then $R(t) \longrightarrow 0$.

This show that (H1) holds.
Thus $X_1^* = (\frac{\Lambda}{\mu}, 0)$ is globally asymptotically stable equilibrium point for the reduced system model equation $\frac{dX_1}{dt} = F(X_1, 0)$.
Next consider

$$\frac{dX_2}{dt} = G(X_1, X_2) = \begin{bmatrix} \beta S(V+I) - (\mu+\omega+q)E \\ \omega E - (\mu+d+\delta+\alpha)I \\ \delta I - (\mu+\rho+\theta+\phi)C_1 \\ \phi C_1 - (\mu+m)C_2 \\ kI - \epsilon V \end{bmatrix}.$$

Then, $\frac{\partial G}{\partial X_2}(X_1, X_2)$

$$= \begin{bmatrix} -(\mu+\omega+q) & \beta S & 0 & 0 \\ \omega & -(\mu+d+\delta+\alpha) & 0 & 0 \\ 0 & \delta & -(\mu+\rho+\theta+\phi) & \theta \\ 0 & 0 & \theta & 0 \\ 0 & k & 0 & 0 \end{bmatrix}$$

$$\begin{bmatrix} 0 & \beta S \\ 0 & 0 \\ 0 & 0 \\ -(\mu+m) & 0 \\ 0 & -\epsilon \end{bmatrix}.$$

Then, $\frac{\partial G}{\partial X_2}(X_1^*, 0)$

$$= \begin{bmatrix} -(\mu+\omega+q) & \beta\frac{\Lambda}{\mu} & 0 & 0 \\ \omega & -(\mu+d+\delta+\alpha) & 0 & 0 \\ 0 & \delta & -(\mu+\rho+\theta+\phi) & \theta \\ 0 & 0 & \theta & 0 \\ 0 & k & 0 & 0 \end{bmatrix}$$

$$= \begin{bmatrix} 0 & \beta\frac{\Lambda}{\mu} \\ 0 & 0 \\ 0 & 0 \\ -(\mu+m) & 0 \\ 0 & -\epsilon \end{bmatrix} = A.$$

This is an M-matrix with non-negatives off diagonal elements. Then, we have
$G(X_1, X_2) = AX_2 - \widehat{G}(X_1, X_2)$,
$\widehat{G}(X_1, X_2) = AX_2 - G(X_1, X_2)$,

$$= \begin{bmatrix} -(\mu+\omega+q) & \beta\frac{\Lambda}{\mu} & 0 & 0 \\ \omega & -(\mu+d+\delta+\alpha) & 0 & 0 \\ 0 & \delta & -(\mu+\rho+\theta+\phi) & \theta \\ 0 & 0 & \theta & 0 \\ 0 & k & 0 & 0 \end{bmatrix}$$

$$\begin{bmatrix} 0 & \beta\frac{\Lambda}{\mu} \\ 0 & 0 \\ 0 & 0 \\ -(\mu+m) & 0 \\ 0 & -\epsilon \end{bmatrix} \begin{bmatrix} E \\ I \\ C_1 \\ C_2 \\ V \end{bmatrix}$$

$$- \begin{bmatrix} \beta S(V+I) - (\mu+\omega+q)E \\ \omega E - (\mu+d+\delta+\alpha)I \\ \delta I - (\mu+\rho+\theta+\phi)C_1 \\ \phi C_1 - (\mu+m)C_2 \\ kI - \epsilon V \end{bmatrix}$$

$$= \begin{bmatrix} \beta(V+I)\left[\frac{\Lambda}{\mu} - S\right] \\ 0 \\ 0 \\ 0 \\ 0 \end{bmatrix}.$$

Since, $0 \le S \le \frac{\Lambda}{\mu}$.
Hence, $\widehat{G}(X_1, X_2) \ge 0$. This show that (H2) holds.

Therefore, provided that $\mathcal{R}_0 < 1$ we can conclude that the infection-free equilibrium point is globally asymptotically stable under these extreme circumstances. □

3.6 Stability of the infected steady state

3.6.1 Local stability of the infected steady state

Theorem 3.5. *When $\mathcal{R}_0 > 1$, the infected steady state point (E_1^*) is stable if it satisfies the Routh-Hurwitz criteria.*

Proof. The Jacobian matrix at the infected steady state is determined as follows:

$J(E_1^*)$

$$= \begin{bmatrix} -[\mu+\beta(V^*+I^*)] & 0 & -\beta S^* & 0 & 0 \\ \beta(V^*+I^*) & -(\mu+\omega+q) & \beta S^* & 0 & 0 \\ 0 & \omega & -(\mu+d+\delta+\alpha) & 0 & 0 \\ 0 & 0 & \delta & 0 & 0 \\ 0 & 0 & 0 & k & 0 \\ 0 & q & \alpha & 0 & 0 \end{bmatrix}$$

$$\begin{bmatrix} 0 & 0 & -\beta S^* & 0 \\ 0 & 0 & \beta S^* & 0 \\ 0 & 0 & 0 & 0 \\ -(\mu+\rho+\theta+\phi) & 0 & 0 & 0 \\ \theta & -(\mu+m) & 0 & 0 \\ 0 & 0 & -\epsilon & 0 \\ \phi & 0 & 0 & -\mu \end{bmatrix}. \quad (3.17)$$

Then, the characteristic equation of Eq. (3.17) is given by

$$\lambda^4 + a_1\lambda^3 + a_2\lambda^2 + a_3\lambda + a_4 = 0,$$

where

$$a_1 = 3\mu + d + \delta + \alpha + \omega + q + \epsilon + \beta(V^* + I^*),$$
$$a_2 = (\mu + \beta(V^* + I^*))(\mu + d + \delta + \alpha) + (\mu + \omega + q + \epsilon)(2\mu + d + \delta + \alpha + \beta(V^* + I^*)) + \epsilon(\mu + \omega + q) - \beta S^* \omega,$$
$$a_3 = (\mu + \omega + q + \epsilon)(\mu + \beta(V^* + I^*))(\mu + d + \delta + \alpha) + \epsilon(\mu + \omega + q)(\mu + \beta(V^* + I^*))(\mu + d + \delta + \alpha) - \beta S^* \omega(k + \mu + \epsilon),$$
$$a_4 = \epsilon(\mu + \omega + q)(\mu + \beta(V^* + I^*))(\mu + d + \delta + \alpha) - \beta S^* \omega \mu(k + \epsilon).$$

Therefore, the infected steady state is stable if it satisfies the Routh-Hurwitz criteria for n = 4, that is

(i) $a_1 > 0, a_3 > 0, a_4 > 0$, and

(ii) $a_1 a_2 a_3 > a_3^2 + a_1^2 a_4$. □

3.6.2 Global stability of the infected steady state

Theorem 3.6. *(global stability of E_1^*). If $\mathcal{R}_0 > 1$, then the infected equilibrium point E_1^* is globally asymptotically stable in Ω.*

Proof. We use the method of Lyapunov functions. We define the positive definite Lyapunov function as

$$L = (S - S^* - S^* \ln \frac{S}{S^*}) + (E - E^* - E^* \ln \frac{E}{E^*}) + (\frac{\mu + \omega + q}{\omega})(I - I^* - I^* \ln \frac{I}{I^*}) + (C_1 - C_1^* - C_1^* \ln \frac{C_1}{C_1^*}) + (\frac{\mu + \rho + \theta + \phi}{\theta})(C_2 - C_2^* - C_2^* \ln \frac{C_2}{C_2^*}).$$

At infected steady state, we have

$$\Lambda = \Big[\mu + \beta(V^* + I^*)\Big]S^*,$$
$$\mu + \omega + q = \frac{\beta S^*(V^* + I^*)}{E^*},$$
$$\mu + d + \delta + \alpha = \frac{\omega E^*}{I^*},$$
$$\mu + \rho + \theta + \phi = \frac{\delta I^*}{C_1^*},$$
$$\mu + m = \frac{\theta C_1^*}{C_2^*}.$$

It can be seen that L is positive definite, and $L(S^*, E^*, I^*, C_1^*, C_2^*, V^*, R^*) = 0$.
Next, calculating the derivative of L along the solutions of the model gives

$$L' = \frac{\partial L}{\partial S} \cdot \frac{dS}{dt} + \frac{\partial L}{\partial E} \cdot \frac{dE}{dt} + \frac{\partial L}{\partial I} \cdot \frac{dI}{dt} + \frac{\partial L}{\partial C_1} \cdot \frac{dC_1}{dt} + \frac{\partial L}{\partial C_2} \cdot \frac{dC_2}{dt},$$

Consider the above in separate terms, and we have

$$\begin{aligned}\frac{\partial L}{\partial S} \cdot \frac{dS}{dt} &= (1 - \frac{S^*}{S})(\Lambda - \mu S - \beta S(V + I)) \\ &= (1 - \frac{S^*}{S})(\mu S^* + \beta S^*(V^* + I^*) - \mu S - \beta S(V + I)) \\ &= \mu S^* \left(2 - \frac{S}{S^*} - \frac{S^*}{S}\right) + \beta S^*(V^* + I^*) \left(1 - \frac{S^*}{S} - \frac{S(V + I)}{S^*(V^* + I^*)} + \frac{V + I}{V^* + I^*}\right),\end{aligned}$$

$$\begin{aligned}\frac{\partial L}{\partial E} \cdot \frac{dE}{dt} &= \left(1 - \frac{E^*}{E}\right)\Big(\beta S(V + I) - (\mu + \omega + q)E\Big) \\ &= \left(1 - \frac{E^*}{E}\right)\Big(\beta S(V + I) - \frac{\beta S^*(V^* + I^*)}{E^*}E\Big) \\ &= \beta S^*(V^* + I^*)\left(1 - \frac{E}{E^*} - \frac{E^* S(V + I)}{E S^*(V^* + I^*)} + \frac{S(V + I)}{S^*(V^* + I^*)}\right),\end{aligned}$$

$$\begin{aligned}\frac{\partial L}{\partial I} \cdot \frac{dI}{dt} &= \left(1 - \frac{I^*}{I}\right)\left(\frac{\mu + \omega + q}{\omega}\right)\Big(\omega E - (\mu + d + \delta + \alpha)I\Big) \\ &= \left(1 - \frac{I^*}{I}\right)\frac{\beta S^*(V^* + I^*)}{\omega E^*}\Big(\omega E - \frac{\omega E^*}{I^*}I\Big)\end{aligned}$$

$$= \beta S^*(V^* + I^*)\left(\frac{E}{E^*} - \frac{I}{I^*} - \frac{EI^*}{E^*I} + 1\right),$$

$$\frac{\partial L}{\partial C_1}\cdot\frac{dC_1}{dt} = \left(1 - \frac{C_1^*}{C_1}\right)\left(\delta I - (\mu+\rho+\theta+\phi)C_1\right)$$
$$= \left(1 - \frac{C_1^*}{C_1}\right)\left(\delta I - \frac{\delta I^*}{C_1^*}C_1\right)$$
$$= \delta I^*\left(1 - \frac{C_1}{C_1^*} - \frac{C_1^* I}{C_1 I^*} + \frac{I}{I^*}\right).$$

And,

$$\frac{\partial L}{\partial C_2}\cdot\frac{dC_2}{dt} = \left(1 - \frac{C_2^*}{C_2}\right)\left(\frac{\mu+\rho+\theta+\phi}{\theta}\right)\left(\theta C_1 - (\mu+m)C_2\right)$$
$$= \left(1 - \frac{C_2^*}{C_2}\right)\left(\frac{\delta I^*}{\theta C_1^*}\right)\left(\theta C_1 - \frac{\theta C_1^*}{C_2^*}C_2\right)$$
$$= \delta I^*\left(\frac{C_1}{C_1^*} - \frac{C_2}{C_2^*} - \frac{C_1 C_2^*}{C_1^* C_2} + 1\right).$$

Hence,

$$L' = \frac{\partial L}{\partial S}\cdot\frac{dS}{dt} + \frac{\partial L}{\partial E}\cdot\frac{dE}{dt} + \frac{\partial L}{\partial I}\cdot\frac{dI}{dt} + \frac{\partial L}{\partial C_1}\cdot\frac{dC_1}{dt} + \frac{\partial L}{\partial C_2}\cdot\frac{dC_2}{dt}$$
$$= \mu S^*\left(2 - \frac{S}{S^*} - \frac{S^*}{S}\right) + \delta I^*\left(2 - \frac{C_2}{C_2^*} - \frac{C_1 C_2^*}{C_1^* C_2} + \frac{I}{I^*}\left(1 - \frac{C_1^*}{C_1}\right)\right)$$
$$+ \beta S^*(V^* + I^*)\left(3 - \frac{S^*}{S} - \frac{I}{I^*} - \frac{EI^*}{E^*I} + \frac{V+I}{V^*+I^*}\left(1 - \frac{E^*S}{ES^*}\right)\right).$$

By the fact that the arithmetic mean is greater than or equal to the geometric mean, we have

$$2 - \frac{S}{S^*} - \frac{S^*}{S} \le 0,$$
$$2 - \frac{C_2}{C_2^*} - \frac{C_1 C_2^*}{C_1^* C_2} + \frac{I}{I^*}\left(1 - \frac{C_1^*}{C_1}\right) \le 0,$$
$$3 - \frac{S^*}{S} - \frac{I}{I^*} - \frac{EI^*}{E^*I} + \frac{V+I}{V^*+I^*}\left(1 - \frac{E^*S}{ES^*}\right) \le 0.$$

This leads $L' < 0$ and $L' = 0$ when $S = S^*, E = E^*, I = I^*, C_1 = C_1^*$ and $C_2 = C_2^*$. By the LaSalle invariance principle [22], the infected steady state E_1^* is globally asymptotically stable when $\mathcal{R}_0 > 1$. □

4. Optimal Control Model

In order to prevent the HPV infection from spreading, we extend the system (2.1) by applying optimal control variables in the model shown in Fig. 2. We include three control variables defined as:
(i) $u_1(t)$ is the preventive vaccine control.
(ii) $u_2(t)$ is the treatment effort for infected cervical cells.
(iii) $u_3(t)$ is the treatment effort for early-stage cervical cancer cells.

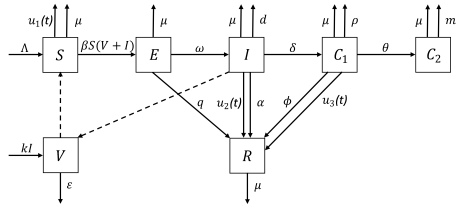

Fig. 2. A schematic diagram for the optimal control model of HPV infection.

The model above can be written as a system of equations as follows:

$$\frac{dS}{dt} = \Lambda - \mu S - \beta S(V+I) - u_1(t)S,$$
$$\frac{dE}{dt} = \beta S(V+I) - (\mu+\omega+q)E,$$
$$\frac{dI}{dt} = \omega E - (\mu+d+\delta+\alpha)I - u_2(t)I,$$
$$\frac{dC_1}{dt} = \delta I - (\mu+\rho+\theta+\phi)C_1 - u_3(t)C_1,$$
$$\frac{dC_2}{dt} = \theta C_1 - (\mu+m)C_2,$$

$$\frac{dV}{dt} = kI - \epsilon V,$$
$$\frac{dR}{dt} = qE + \alpha I + \phi C_1 - \mu R + u_2(t)I + u_3(t)C_1. \quad (4.1)$$

The objective of the optimal control model is to minimize the number of exposed cervical cells, infected cervical cells, early-stage cervical cancer cells, end-stage cervical cancer cells and human papillomavirus (HPV) at a minimal cost of control over the time interval $[0, T]$, i.e.

$$P(u_1, u_2, u_3) = \min \int_0^T \Big[A_1E + A_2I + A_3C_1 + A_4C_2 + A_5V + \frac{1}{2}(A_6u_1^2(t) + A_7u_2^2(t) + A_8u_3^2(t)) \Big] dt \quad (4.2)$$

with initial conditions

$S(0) \geq 0,\ E(0) \geq 0,\ I(0) \geq 0,\ C_1(0) \geq 0,\ C_2(0) \geq 0,\ V(0) \geq 0$ and $R(0) \geq 0$.

Here the weight constants are $A_1, A_2, A_3, A_4, A_5, A_6, A_7$ and A_8 and the terms $A_6u_1^2(t)$, $A_7u_2^2(t)$ and $A_8u_3^2(t)$ represent the costs associated with preventive vaccines control, the treatment effort for infected cervical cells and treatment effort for early-stage cervical cancer cells, respectively.

The Lagrangian of the optimal control problem is given by

$$g(E, I, C_1, C_2, V, u_1, u_2, u_3) = A_1E + A_2I + A_3C_1 + A_4C_2 + A_5V + \frac{1}{2}\big[A_6u_1^2(t) + A_7u_2^2(t) + A_8u_3^2(t)\big]. \quad (4.3)$$

Applying Pontryagin's Minimum Principle (PMP), we form the Hamiltonian and derive the optimality system:

$$\begin{aligned} H &= A_1E + A_2I + A_3C_1 + A_4C_2 + A_5V \\ &+ \frac{1}{2}\big[A_6u_1^2(t) + A_7u_2^2(t) + A_8u_3^2(t)\big] \\ &+ \lambda_S[\Lambda - \mu S - \beta S(V + I) - u_1(t)S] \\ &+ \lambda_E[\beta S(V + I) - (\mu + \omega + q)E] \\ &+ \lambda_I[\omega E - (\mu + d + \delta + \alpha)I - u_2(t)I] \\ &+ \lambda_{C_1}[\delta I - (\mu + \rho + \theta + \phi)C_1 - u_3(t)C_1] \\ &+ \lambda_{C_2}[\theta C_1 - (\mu + m)C_2] + \lambda_V[kI - \epsilon V] \\ &+ \lambda_R[qE + \alpha I + \phi C_1 - \mu R + u_2(t)I + u_3(t)C_1], \end{aligned} \quad (4.4)$$

where $\lambda_S, \lambda_E, \lambda_I, \lambda_{C_1}, \lambda_{C_2}, \lambda_V$ and λ_R are the adjoint functions associated with the state equations for S, E, I, C_1, C_2, V and R, respectively.

Theorem 4.1. *Let $\widetilde{S}, \widetilde{E}, \widetilde{I}, \widetilde{C_1}, \widetilde{C_2}, \widetilde{V}$ and $\widetilde{R}$ be optimal state solution with associated optimal control variable $u_1^*(t)$, $u_2^*(t)$ and $u_3^*(t)$ for the optimal control problem of the system* (4.1). *Then there exist adjoint variables $\lambda_S, \lambda_E, \lambda_I, \lambda_{C_1}, \lambda_{C_2}, \lambda_V$ and λ_R satisfying:*

$$\begin{aligned} \lambda_S' &= -\Big[-\lambda_S\Big(u_1(t) + \mu + \beta(\widetilde{V} + \widetilde{I})\Big) + \lambda_E\Big(\beta(\widetilde{V} + \widetilde{I})\Big)\Big], \\ \lambda_E' &= -\Big[A_1 - \lambda_E(\mu + \omega + q) + \lambda_I\omega + \lambda_R q\Big], \\ \lambda_I' &= -\Big[A_2 - \lambda_S\beta\widetilde{S} + \lambda_E\beta\widetilde{S} - \lambda_I\Big((\mu + d + \delta + \alpha) + u_2(t)\Big) + \lambda_{C_1}\delta + \lambda_V k + \lambda_R\Big(u_2(t) + \alpha\Big)\Big], \\ \lambda_{C_1}' &= -\Big[A_3 - \lambda_{C_1}\Big((\mu + \rho + \theta + \phi) + u_3(t)\Big) + \lambda_{C_2}\theta + \lambda_R\Big(\phi + u_3(t)\Big)\Big], \\ \lambda_{C_2}' &= -\Big[A_4 - \lambda_{C_2}(\mu + m)\Big], \\ \lambda_V' &= -\Big[A_5 - \lambda_S\beta\widetilde{S} + \lambda_E\beta\widetilde{S} - \lambda_V\epsilon\Big], \end{aligned}$$

$$\lambda_R^{'} = -\Big[- \lambda_R \mu \Big].$$

with transversality conditions:

$$\lambda_S(T) = 0, \lambda_E(T) = 0, \lambda_I(T) = 0, \lambda_{C_1}(T) = 0,$$
$$\lambda_{C_2}(T) = 0, \lambda_V(T) = 0, \lambda_R(T) = 0.$$

And, the characterization of the optimal control is given by

$$u_1^*(t) = \max\{0, \min(u_{1\max}, u_1)\},$$
$$u_2^*(t) = \max\{0, \min(u_{2\max}, u_2)\},$$
$$u_3^*(t) = \max\{0, \min(u_{3\max}, u_3)\},$$

where

$$u_1 = \frac{\lambda_S \widetilde{S}}{A_6},$$
$$u_2 = \frac{(\lambda_I - \lambda_R)\widetilde{I}}{A_7},$$
$$u_3 = \frac{(\lambda_{C_1} - \lambda_R)\widetilde{C_1}}{A_8}.$$

Proof. We first differentiate the Hamiltonian with respect to S, E, I, C_1, C_2, V and R, respectively, and then the adjoint system is obtained as follows:

$$\lambda_S^{'} = -\frac{\partial H}{\partial S} = -\Big[- \lambda_S \Big(u_1(t) + \mu + \beta(\widetilde{V} + \widetilde{I})\Big) + \lambda_E \beta(\widetilde{V} + \widetilde{I})\Big],$$
$$\lambda_E^{'} = -\frac{\partial H}{\partial E} = -\Big[A_1 - \lambda_E(\mu + \omega + q) + \lambda_I \omega + \lambda_R q\Big],$$
$$\lambda_I^{'} = -\frac{\partial H}{\partial I} = -\Big[A_2 - \lambda_S \beta \widetilde{S} + \lambda_E \beta \widetilde{S} - \lambda_I \Big((\mu + d + \delta + \alpha) + u_2(t)\Big) + \lambda_{C_1}\delta + \lambda_V k + \lambda_R \Big(u_2(t) + \alpha\Big)\Big],$$
$$\lambda_{C_1}^{'} = -\frac{\partial H}{\partial C_1} = -\Big[A_3 - \lambda_{C_1}\Big((\mu + \rho + \theta + \phi) + u_3(t)\Big) + \lambda_{C_2}\theta + \lambda_R\Big(\phi + u_3(t)\Big)\Big],$$
$$\lambda_{C_2}^{'} = -\frac{\partial H}{\partial C_2} = -\Big[A_4 - \lambda_{C_2}(\mu + m)\Big],$$
$$\lambda_V^{'} = -\frac{\partial H}{\partial V} = -\Big[A_5 - \lambda_S \beta \widetilde{S} + \lambda_E \beta \widetilde{S} - \lambda_V \epsilon\Big],$$
$$\lambda_R^{'} = -\frac{\partial H}{\partial R} = -\Big[- \lambda_R \mu\Big]. \tag{4.5}$$

Further, by the approach of Pontryagin et al. [23] we solve the equation, $\frac{\partial H}{\partial u_i} = 0$ at u_i^*; for $i = 1, 2, 3$ and we have

$$\frac{\partial H}{\partial u_1} = A_6 u_1(t) - \lambda_S \widetilde{S}$$
$$\therefore u_1(t) = \frac{\lambda_S \widetilde{S}}{A_6}. \tag{4.6}$$
$$\frac{\partial H}{\partial u_2} = A_7 u_2(t) + \lambda_R \widetilde{I} - \lambda_I \widetilde{I} = 0$$
$$\therefore u_2(t) = \frac{(\lambda_I - \lambda_R)\widetilde{I}}{A_7}. \tag{4.7}$$
$$\frac{\partial H}{\partial u_3} = A_8 u_3(t) + \lambda_R \widetilde{C_1} - \lambda_{C_1}\widetilde{C_1} = 0$$
$$\therefore u_3(t) = \frac{(\lambda_{C_1} - \lambda_R)\widetilde{C_1}}{A_8}. \tag{4.8}$$

With the standard control arguments involving the bounds on the controls, thus we have

$$u_1^*(t) = \max\left\{0, \min\left\{\frac{\lambda_S \widetilde{S}}{A_6}, u_{1\max}\right\}\right\}, \tag{4.9}$$
$$u_2^*(t) = \max\left\{0, \min\left\{\frac{(\lambda_I - \lambda_R)\widetilde{I}}{A_7}, u_{2\max}\right\}\right\}, \tag{4.10}$$
$$u_3^*(t) = \max\left\{0, \min\left\{\frac{(\lambda_{C_1} - \lambda_R)\widetilde{C_1}}{A_8}, u_{3\max}\right\}\right\}. \tag{4.11}$$

This completes the proof. □

5. Numerical Simulation of Optimal Control Problem

In this section, the dynamics of the system (4.1) are studied by performing numerical simulations. We use the forward-

backward sweep method to solve the optimality system numerically. We consider the optimal control continuously for 15 years, with the use of parameter values in Table 1. The numerical results are shown in Figs. 3-6. We divide our results into four startegies as shown below, where the solid line and the dash line represents control and non-control condition, respectively.

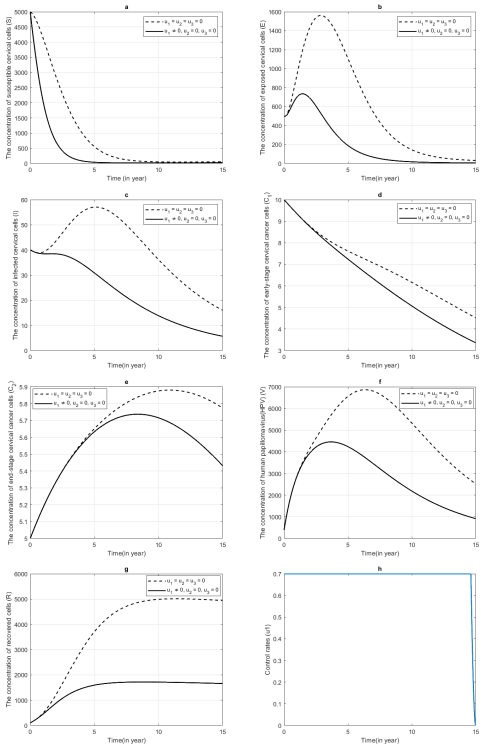

Fig. 3. Numerical simulation of the optimal control model (4.1) with optimal control of preventive vaccines of u_1 alone when $u_{1max} = 0.7$. (a-g) the concentration of S, E, I, C_1, C_2, V and R, and (h) the strategy guildline of control (u_1).

5.1 Strategy A : Control with the preventive vaccines control only

Under this strategy, we use control u_1 to optimize the objective function while u_2 and u_3 are set to be zero. Fig. 3(a) shows that the concentration of susceptible cervical cells (S) reduces faster in the control condition and seems to reach equilibrium value faster than non-control one. Fig. 3(b) shows that the concentration of exposed cervical cells (E) decreases significantly in control case, whereas it reaches the peak of more than 1,580 $cells/mm^3/year$ in non-control one. Further, the result shows that it reaches the equilibrium value faster in the control condition. Fig. 3(c) shows that the concentration of infected cervical cells (I) reduces dramatically in the control case since the start, whereas it increases and reaches the peak of 57 $cells/mm^3/year$ in the non-control one. Fig. 3(d) shows that in control case the concentration of early-stage cervical cancer cells (C_1) reduces faster and more than non-control case. Figs.3 (e-g) show that in control condition, the concentration of end-stage cervical cancer cells (C_2), the concentration of human papillomavirus (HPV) (V) and the concentration of recovered cells (R), respectively, reduce significantly and tends to reach lower value of equilibrium state. From the results above, it is obtained that u_1 could have a big impact in reducing the concentration of E, I, C_1, C_2, V and R. Finally, Fig. 3(h) shows the strategy of u_1 that it has to be at the maximum rate of 70% for about 14 years and then decreases gradually towards zero in the 15^{th} year.

5.2 Strategy B : Control with the treatment effort for infected cervical cells control only

Under this strategy, we use control u_2 to optimize the objective function while u_1 and u_3 are set to be zero. Fig. 4(a) shows that the concentration of susceptible cervical cells (S) reduces slower in the control condition and seems to reach higher equilibrium value than the non-control one. Fig. 4(b) shows that the concentration of exposed cervical cells (E) decreases in

Table 1. Parameter values used in the model.

Parameter	Description	Value	Unit	Reference
Λ	The constant recruitment rate of cervical cells	20	$cells/mm^3/year$	Estimated
β	The infection rate	0.0001	mm^3	Gureu, E.D., 2019
ω	The progression rate from exposed cervical cells to infected cervical cells	0.01	$year$	Asih, T.S.N., 2016
q	The recovery rate of exposed cervical cells	0.6	$year^-1$	Gureu, E.D., 2019
d	The death rate of infected cervical cells due to the HPV infection	0.15	$year^-1$	Gureu, E.D., 2019
δ	The progression rate from infected cervical cells to early-stage cervical cancer cells	0.0082	$year^-1$	Asih, T.S.N., 2016
α	The recovery rate of infected cervical cells	0.02	$year^-1$	Estimated
ρ	The death rate of early-stage cervical cancer cells due to cancer	0.04	$year^-1$	Estimated
θ	The progression rate from early-stage cervical cancer cells to end-stage cervical cancer cells	0.04	$year^-1$	Gureu, E.D., 2019
ϕ	The recovery rate of early-stage cervical cancer cells due to treatment	0.01	$year^-1$	Kheunchana, R., 2020
m	The death rate of end-stage cervical cancer cells due to cancer	0.03	$year^-1$	Gureu, E.D., 2019
μ	The natural death rate of cervical cells	0.01	$year^-1$	Kheunchana, R., 2020
k	The HPV generated rate which are produced by the infected cervical cells	100	$year^-1$	Estimated
ϵ	The clearance rate of HPV	0.8	$year^-1$	Estimated

control case with the peak of about 1,075 $cells/mm^3/year$, whereas it reaches the peak of more than 1,580 $cells/mm^3/year$ in non-control one. Fig. 4(c) shows that the concentration of infected cervical cells (I) reduces considerably in the control case since the start, whereas it increases and reaches the peak of 57 $cells/mm^3/year$ in non-control one. Fig. 4(d) shows that in control case the concentration of early-stage cervical cancer cells (C_1) reduces faster and more than the non-control case and seems to reach lower equilibrium value. Fig. 4(e) shows that in control condition, the concentration of end-stage cervical cancer cells (C_2) increases, reaches the peak and drops down faster than the non-control one. Fig. 4(f) shows a significant reduction of the concentration of human papillomavirus (HPV) (V) in control case, and the peak in the control case occurs much faster. Further, with control, it tends to reach much lower equilibrium value. Fig. 4(g) shows that in control condition, the concentration of recovered cells (R) reduces largely and tends to reach lower value of equilibrium state. Finally, Fig. 4(h) shows the strategy of u_2 that it has to start at the maximum

rate of 70% for about 14 years and gradually goes down to 0 on the 15^{th} year. Further, from the results above, it is obtained that u_2 could have a big impact in reducing the concentration of E, I, C_1, C_2 and V.

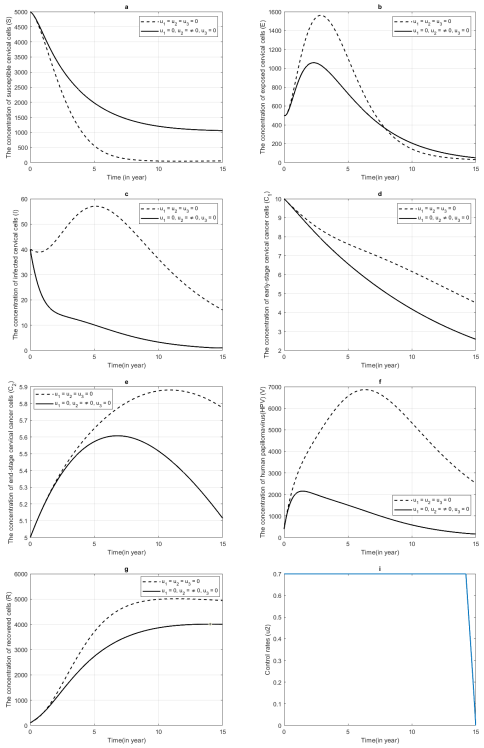

Fig. 4. Numerical simulation of the optimal control model (4.1) with optimal control of treatment effort of infected cervical cells of u_2 alone when $u_{2max} = 0.7$. (a-g) the concentration of S, E, I, C_1, C_2, V and R, and (i) the strategy guildline of control (u_2).

5.3 Strategy C : Control with the treatment effort for early-stage cervical cancer cells control only

Under this strategy, we use control u_3 to optimize the objective function while u_1 and u_2 are set to be zero. With this strategy, Figs. 5(a-c, f, g) demonstrate an unchange in the concentration of susceptible cervical cells (S), the concentration of exposed cervical cells (E), the concentration of infected cervical cells (I), the concentration of human papillomavirus (HPV) (V) and the concentration of recovered cells (R) between the control and the non-control one. However, Figs. 5(d-e) show a dramatic decrease in the concentration of early-stage cervical cancer cells (C_1) and the concentration of end-stage cervical cancer cells (C_2) in the control case comparing to the non-control one. From the results above, it is obtained that (u_3) plays a key role only in reducing the concentration of early-stage cervical cancer cells (C_1) and the concentration of end-stage cervical cancer cells (C_2). Finally, Fig. 5(h) shows the strategy of u_3 that it has to start at the maximum rate of 70% for about 10 years and 4 months and goes down to 0 at the 15^{th} year.

5.4 Strategy D : Combination of all controls

Under this strategy, we use a combination of all three controls to optimize the objective fuction. Fig. 6(a) shows that the concentration of susceptible cervical cells (S) reduces faster in the control condition and seems to reach equilibrium value faster than the non-control one. Fig. 6(b) shows that the concentration of exposed cervical cells (E) decreases significantly in the control case, whereas it reaches the peak of more than 1,580 $cells/mm^3/year$ in the non-control one. Further, the result shows that the peak occurs faster and it reaches the equilibrium value faster in the control condition. Fig. 6(c) shows that the concentration of infected cervical cells (I) reduces considerably in the control case since the start, whereas it increases and reaches the peak of 57 $cells/mm^3/year$ in non-control one. Fig. 6(d-e) show dramatic decrease in the concentration of early-stage cervical cancer cells (C_1) and the concentration of end-stage cervical cancer cells (C_2) in

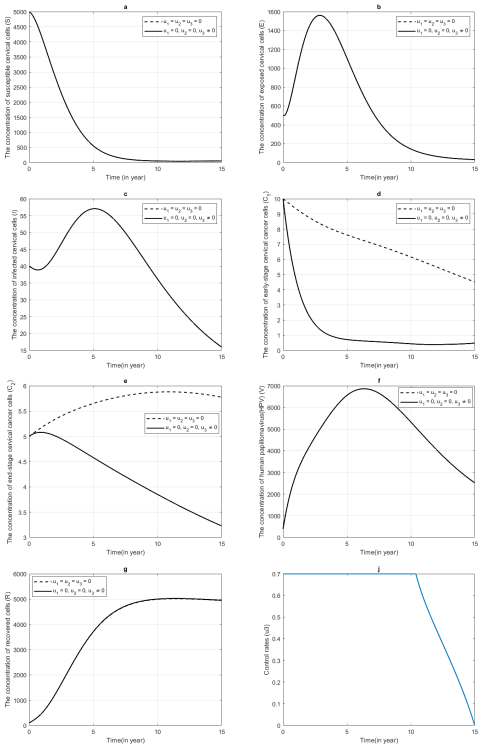

Fig. 5. Numerical simulation of the optimal control model (4.1) with optimal control of preventive and treatment effort of early-stage cervical cancer cells of u_3 alone when $u_{3max} = 0.7$. (a-g) the concentration of S, E, I, C_1, C_2, V and R, and (j) the strategy guildline of control (u_3).

control case comparing to non-control one. Fig. 6(f) shows a significant reduction of the concentration of human papillomavirus (HPV) (V) in the control case and it reaches the peak much faster than the non-control one. Fig. 6(g) shows that in the control condition, the concentration of recovered cells (R) reduce largely and tends to reach lower value of equilibrium state.

Overall, our results demonstrate that u_1 seems to give an impact in reducing the concentration of S, E, I, C_1, C_2, V and R. The control u_2 gives an impact mainly in reducing the concentration of E, I, C_1, C_2 and V whereas the control u_3 only gives impact mainly in decreasing the value of C_1 and C_2. However, a combination of all three controls give the best result in reducing the HPV infection of cervical epithelial cells overall.

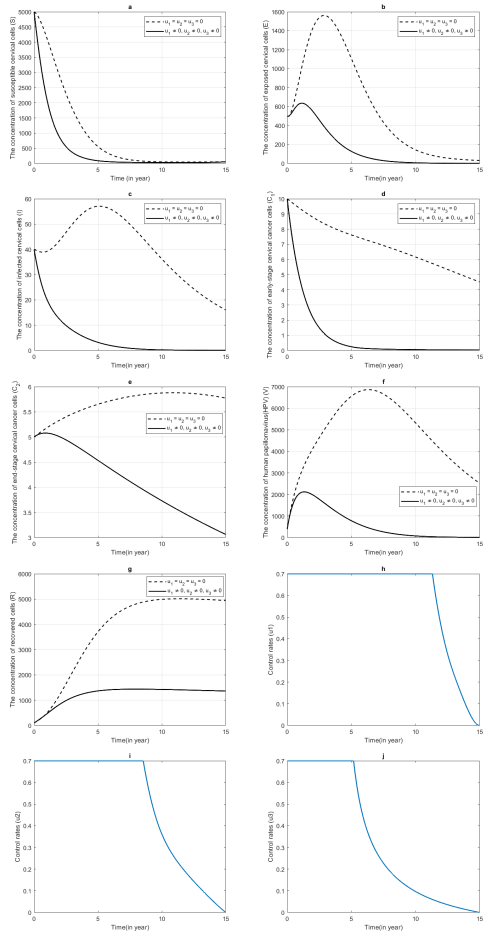

Fig. 6. Numerical simulation of the optimal control model (4.1) with optimal control of antiretroviral therapy of u_1, u_2 and u_3 when $u_{1max} = u_{2max} = u_{3max} = 0.7$. (a-g) the concentration of S, E, I, C_1, C_2, V and R, and (h)-(j) the strategy guildeline of control (u_1), (u_2) and (u_3).

6. Conclusions

Although HPV vaccine has been available in many countries worldwide, there are still a number of infected people with HPV and cervical cancer, and they

have been increasing in the past decade. A kinetic of virus spreading within cells therefore remains essential to understand. In this paper, we propose a within-host model of HPV infection and cervical cancer. We extend the work of Asih et al. [16] by adding the latent period of HPV infection and the recovery state of cells. There are seven compartments in this model consists of S is the concentration of susceptible cervical cells, E is the concentration of exposed cervical cells, I is the concentration of infected cervical cells, C_1 is the concentration of early-stage cervical cancer cells, C_2 is the concentration of end-stage cervical cancer cells, V is the concentration of human papillomavirus (HPV) and R is the concentration of recovered cells. All model properties are demonstrated starting from the existence, positivity and boundary of solutions. Two equilibrium points which are infection-free and infected steady state are determined. The basic reproduction number is calculated using next generation method and it becomes the threshold for stability of equilibrium points i.e., when it is less than unity, the infection-free equilibrium point is both locally and globally stable whereas when it is greater than one the infection persists and the infected steady state is globally stable. Further, an optimal control problem by Pontryagin's Minimum Principle is applied into the model with three control variables consisting of preventive control, treatment effort for infected cervical cells and treatment effort for early-stage cervical cancer cells. The numerical simulations of optimal control model are performed and the results demonstrate that vaccines could reduce HPV infection and cervical cancer greatly. The treatment effort for early-stage cervical cancer cells could significantly decrease the concentration of infected cervical cells and viruses and the treatment effort for end-stage cervical cancer cells mainly reduces the concentration of both stages of cancer cells. However, with a combination of all three controls we obtain the best solution in reducing the HPV infection and cervical cancer overall. These results confirm an encouragement in having vaccine and treatment once one getting infected as early as possible.

Acknowledgments

This work has been supported by Department of Mathematics, Faculty of Science, Naresuan University, Thailand.

References

[1] Burd EM. Human papillomavirus and cervical cancer. Clinical Microbiology Reviews, 2003;16(1):1-17.

[2] Chan CK, Aimagambetova G, Ukybassova T, Kongrtay K, Azizan A. Human papillomavirus infection and cervical cancer: epidemiology, screening, and vaccination-review of current perspectives. Journal of Oncology, 2019; 3257939.

[3] Meites E, Gee J, Under E, Markowitz L. Human papillomavirus. Centers for Disease Control and Prevention. Available from: https://www.cdc.gov/vaccines/pubs/pinkbook/hpv.html#hpv

[4] Mirabello L, Clarke MA, Nelson CW, Dean M, Wentzensen N, Yeager M, Cullen M, Boland JF, Schiffman M, Burk RD. The intersection of HPV epidemiology, genomics and mechanistic studies of HPV-mediated carcinogenesis. Viruses, 2018;10(2).

[5] Ryser MD, Gravitt PE, Myers ER. Mechanistic mathematical models: an underused platform for HPV research. Papillomavirus Research, 2017;3:46-9.

[6] WHO. Cervical cancer. Available from https://www.who.int/news-room/fact-sheets/detail/cervical-cancer

[7] Brotherton JML. Impact of HPV vaccination: achievements and future challenges. Papillomavirus Research, 2019;7:138-40.

[8] Tanaka H, Shirasawa H, Shimizu D, Sato N, Ooyama N, Takahashi O, Terada Y. Preventive effect of human papillomavirus vaccination on the development of uterine cervical lesions in young Japanese women. Journal of Obstetrics and Gynaecology Research, 2017;43(10):1597-601.

[9] Elbasha EH. Global stability of equilibria in a two-sex HPV vaccination model. Bulletin of Mathematical Biology, 2008;70:894-909.

[10] Ribassin-Majed L, Lounes R. A SIS model for human papillomavirus transmission. HAL open science 2010; hal-00555733.

[11] Lee SL, Tameru AM. A mathematical model of human papillomavirus (HPV) in the United States and its impact on cervical cancer. Journal of cancer, 2012;3:262-68.

[12] Gurmu ED, Kumsa B, Koya PR. Optimal control strategy on human papillomavirus (HPV) model with backward bifurcation analysis. IOSR Journal of Mathematics, 2019;15(6):65-87.

[13] Zhang K, Ji Y, Pan Q, Wei Y, Ye Y, Liu H. Sensitivity analysis and optimal treatment control for a mathematical model of human papillomavirus infection. AIMS Mathematics, 2020a;5(3):2646-70.

[14] Zhang K, Wang X, Liu H, Ji Y, Pan Q, Wei Y, Ma M. Mathematical analysis of a human papillomavirus transmission model with vaccination and screening. Mathematical Biosciences and Engineering, 2020b;17(5):5449-76.

[15] Smith RJ, Li J, Mao J, Sahai B. Using within-host mathematical modelling to predict the long-term outcome of human papillomavirus vaccines. Canadian Applied Mathematics Quarterly, 2013;21(2):281-99.

[16] Asih TSN, Lenhart S, Wise S, Aryati L, Adi-Kusumo F, Hardianti MS, Forde J. The dynamics of HPV infection and cervical cancer cells. Bulletin of Mathematical Biology, 2016;78:4-20.

[17] Gurmu ED, Koya PR. Sensitivity analysis and modeling the impact of screening on the transmission dynamics of human papilloma virus (HPV). American Journal of Applied Mathematics, 2019;7(3):70-9.

[18] Allali K. Stability analysis and optimal control model of HPV infection model with early-stage cervical cancer. BioSystems 2021;199:104321.

[19] Mac Indoe E. Analysis of detenministic and stochastic HIV models. Student Research Submissions, 2019:8-9.

[20] van den Drissche P, Watmough J. Reproductive numbers and sub-threshold endemic equilibria for compartment models of disease transmission. Math Biosci, 2002;180:29-48.

[21] Castillo-Chavez C, Feng Z, Huang W. On the Computation of R_0 and its Role on Global Stability. Springer-Verlag and Berlin-Heidelberg-New York,2002:229-50.

[22] La salle, J. P. The Stability of Dynamical Systems, Regional Conference Series in Applied Mathematics, SIAM, Philadelphia, 1976.

[23] Pontryagin LSV, Boltyanskii GR, Gamkrelidze V, Mishchenko EF. The mathematical theory of optimal processes, Gordon and Breach Science, New York, 1986.

[24] Kheunchana R. Mathematical model and optimal control model of HPV infection of epithelial cell in the cervix with vaccination and treatment [Undergraduate thesis]. Phitsanulok: Naresuan University; 2020.